Autoresonance microwave accelerator

R. Shpitalnik, C. Cohen, F. Dothan, and L. Friedland
Center for Plasma Physics, Racah Institute of Physics, Hebrew University of Jerusalem, 91904, Jerusalem, Israel

(Received 10 October 1990; accepted for publication 5 March 1991)

A novel autoresonance acceleration scheme comprising a traveling electromagnetic wave and a magnetostatic field is discussed. A spatially tailored magnetostatic field keeps the electron in a constant phase and allows continuous acceleration. Numerical results are presented. Experimental results, showing acceleration from an initial value of 10 keV to energies of about 150 keV after 1.5 m by using a pulsed 50-kW peak power transmitter, are presented.

I. INTRODUCTION

The theory and experimental techniques of the autoresonance regime are receiving wide attention, since they appear to explain a wide range of physical effects. Special interest is given to acceleration applications. The autoacceleration of charted particles is discussed by a growing number of researchers, e.g., McDermott, Furuno, and Luhmann, Jr.,[1] and Golovanivsky[2–4] who has proposed acceleration by means of standing waves or a time-varying magnetic field.

The autoacceleration of charged particles by traveling waves in an axial magnetic field requires that the Doppler-shifted cyclotron resonance frequency slip be constant. The frequency slip is given by $\Omega/\gamma - (\omega - \mathbf{k}\cdot\mathbf{v})$, where Ω is the charged particle gyrofrequency, ω is the wave radian frequency, $\mathbf{k}$ is the wave vector, and γ and $\mathbf{v}$ are the particle's Lorentz energy factor and velocity, respectively. In a previous paper[5] a standing-wave acceleration scheme has been presented. However, a considerable obstacle in employing such an approach is the fact that most of the energy is contained in the azimuthal velocity component. The second serious problem is the very steep magnetic-field gradient, to be provided in the standing-wave acceleration scheme. As will be shown here, and as has been seen also in related works,[6,7] most of the energy in the present scheme is stored in the axial component of the velocity.

We present here a new approach, in which electrons are accelerated by traveling electromagnetic (EM) waves. In this design, long-distance continuous acceleration makes it possible to avoid focusing problems characteristic of standing-wave acceleration schemes.[5] It also becomes possible to obtain azimuthal bunching and consider coherent synchrotron radiation phenomena.

In this paper we present both the theory of the traveling-wave accelerator and the results achieved on the proof-of-principle experimental system at the Hebrew University of Jerusalem.

II. THEORETICAL MODEL

Consider a cold electron beam propagating along the axis z of a cylindrical waveguide with an axial velocity (at $z=0$) purely in the axial direction. Suppose also that a circularly polarized traveling wave (the TE-11 mode) is excited in the waveguide and propagates along the direction of the beam. Also, assume that the whole system is immersed in a static, axisymmetric guide magnetic field $\mathbf{B}_0$, which may be slowly varied along the axis of the propagation of the beam. Thus, we consider the guided beam transport in the presence of the electromagnetic field, components of which are in cylindrical coordinates:

$$\begin{aligned} E_r &= (2E)(1/\sigma r)J_1(\sigma r)\cos\alpha, \\ E_\theta &= -(2E)J_1'(\sigma r)\sin\alpha, \\ B_r &= (2E)(ck/\omega)J_1'(\sigma r)\sin\alpha, \\ B_\theta &= (2E)(ck/\omega)(1/\sigma r)J_1(\sigma r)\cos\alpha, \\ B_z &= (2E)(c\sigma/\omega)J_1(\sigma r)\cos\alpha, \end{aligned} \tag{1}$$

where E is the electric-field strength on the axis, $\alpha = (\omega t - kz) - (\theta + \pi/2)$, $ck = [\omega^2 - (c\sigma)^2]^{1/2}$, R is the waveguide radius, $J_1(\sigma r)$ is the Bessel function of the first kind, $\sigma = S_{11}/R$, and $S_{11} = 1.841$ is the first zero of $J_1'(\sigma r)$.

At this stage we observe that for $\sigma r < 1$, i.e., when $r < R/S_{11}$ we can limit our analysis to a much simpler electromagnetic-field model. If $\sigma r < 1$, $J_1(\sigma r)$ is almost a linear function. Indeed,

$$J_1(x) = (x/2) + \Delta, \tag{2}$$

where for $x \ll 1$, $\Delta \sim 0(x^3)$, but even for $x = 1$, $\Delta \approx 0.1$. Thus, in the above-mentioned case ($r < R/S_{11}$) the transverse field components are well approximated by a plane wave with

$$\begin{aligned} &E_r = E\cos\alpha, \quad E_\theta = -E\sin\alpha, \\ &B_r = (ck/\omega)E\sin\alpha, \quad B_\theta = (ck/\omega)E\cos\alpha, \end{aligned} \tag{3}$$

or, in the Cartesian coordinates,

$$\begin{aligned} \mathbf{E} &= -E(\hat{e}_x\sin\alpha - \hat{e}_y\cos\alpha), \\ \mathbf{B} &= -(ck/\omega)E(\hat{e}_x\cos\alpha + \hat{e}_y\sin\alpha). \end{aligned} \tag{4}$$

This electromagnetic field will be adopted in the following model. Note that we neglected the B_z component of the field, since this component is assumed to be much smaller than the guide field, $E \ll B_0$.

 0021-8979/91/031101-06$03.00

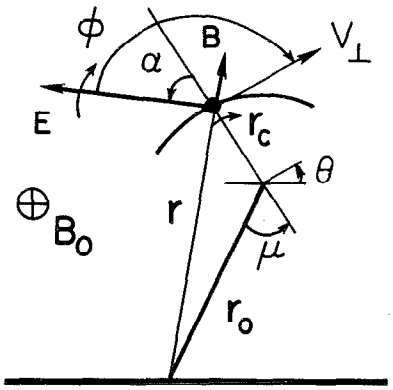

FIG. 1. Electron trajectory projection onto the transverse plane. R_c is the radius of the curvature in the transverse plane at the electron position (r,φ).

Now, we proceed to the equations describing the motion of a particular electron in the beam. In deriving these equations, we decompose the electron velocity vector into the axial and transverse components $\mathbf{v}=\mathbf{v}_\perp + v_z\hat{e}_z$, and define the angle φ between the directions $\mathbf{v}_\perp$ and $\mathbf{E}$. A small segment of the transverse projection of the electron trajectory is shown in Fig. 1. We see in this figure that the transverse acceleration of the electron can be written as

$$m\gamma v_\perp^2/R_c = eE\sin\varphi - (ev_z/c)B\sin\varphi - (e/c)v_\perp B_0, \tag{5}$$

where we have neglected the term on right-hand side due to the radial component of the guided field $\mathbf{B}_0$. This term can be estimated as

$$\frac{ev_z}{2c}r_0\sin\mu\left(\frac{\partial B_0}{\partial z}\right),$$

where $r_0=|\mathbf{r}_0|$ is the gyrocenter radial coordinate and μ is the angle between the gyroradius $\mathbf{R}_c$ vector and $\mathbf{r}_0$ (see Fig. 1). Obviously, this term is canceled out after averaging over the fast gyromotion and we remain with Eq. (5).

The axial electron momentum $m\gamma v_z$ is governed by

$$\frac{md(\gamma v_z)}{dt} = -\frac{ev_\perp}{c}B\cos\varphi - \frac{m}{2}\gamma v_\perp^2\left(\frac{\partial B_0}{\partial z}\right)\frac{1}{B_0}, \tag{6}$$

where the second term on the rhs of Eq. (6) again comes from the radial component of the axial magnetic field.

Finally, the energy factor γ varies according to

$$mc^2\frac{d\gamma}{dt} = -eEv_\perp\cos\varphi. \tag{7}$$

At this point we use Eq. (5) to write an expression for the angular velocity,

$$\Omega=\frac{v_\perp}{R_c}=\frac{eE}{m\gamma v_\perp}\left(1-\frac{k}{\omega}v_z\right)\sin\varphi-\frac{\Omega_c}{\gamma}, \tag{8}$$

where $\Omega_c = eB_0/mc$ is the cyclotron gyrofrequency. The time evolution of the angle φ may be written as

$$\frac{d\varphi}{d\tau}=\frac{d}{d\tau}(kz-w\tau)-\Omega'$$

$$=\left(k\beta_z - w + \frac{\Omega_c'}{\gamma}\right) - \frac{A}{\gamma\beta_\perp}\left(1-\frac{\beta_z}{\beta_P}\right)\sin\varphi, \tag{9}$$

where the notations

$$\tau=tc,\quad w=\omega/c,\quad \beta=\mathbf{v}/c,$$

$$\Omega'=\Omega/c,\quad \Omega_c'=eB_0/mc^2,\quad A=eE/mc^2$$

are used for convenience and $\beta_p = w/k$ is the phase velocity of the wave.

Thus, the electrons of the beam are described by the following set of equations:

$$\dot{\gamma} = -A\beta_\perp\cos\varphi, \tag{10}$$

$$\dot{\varphi} = [k\beta_z - w - (\Omega_c'/\gamma)] - (A/\beta_\perp\gamma)$$

$$\times[1-(\beta_z/\beta_P)]\sin\varphi, \tag{11}$$

$$(\gamma\beta_z)^{\cdot} = -(\beta_\perp/\beta_P)A\cos\varphi - \tfrac{1}{2}(\dot{\Omega}_c'/\Omega_c')\,\gamma(\beta_\perp^2/\beta_z), \tag{12}$$

which, combined with

$$\beta_\perp=(1-\gamma^{-2}-\beta_z^2)^{1/2} \tag{13}$$

and an additional externally imposed (by varying B_0 along the z axis) condition

$$\Omega_c'=w\gamma - k\beta_z\gamma, \tag{14}$$

comprise a complete system of equations describing the beam propagation in the system. We observe now that because of condition (14) and since $\beta_p > 0$, in our case, the factor multiplying $\sin\varphi$ in Eq. (11) is positive, so that if $\beta_\perp$ is sufficiently small this equation describes a rapid convergence of the phase φ towards π.

More generally, one may state that the phase bunching process occurs for

$$\Omega_c' < [(A/\beta_\perp) + w\gamma][1-(\beta_z/\beta_P)], \tag{15}$$

for $\beta_\perp \neq 0$. This assumption is satisfied for values of φ such that

$$\varphi > \sin^{-1}(\beta_\perp/A\{[\Omega_c'/(1-n\beta_z)] - w\gamma\}), \tag{16}$$

where

$$n=1/\beta_p=k/w.$$

After the rapid phase bunching $\varphi\to\pi$, the electrons of the beam enter the positive acceleration stage described by [see Eq. (10)]

$$\dot{\gamma} = A\beta_\perp. \tag{17}$$

In order to maintain this monotonic acceleration mode, we must confine φ to the vicinity of the value $\varphi=\pi$. This confinement can be achieved by requiring that condition (14) is preserved along the axis of the system.

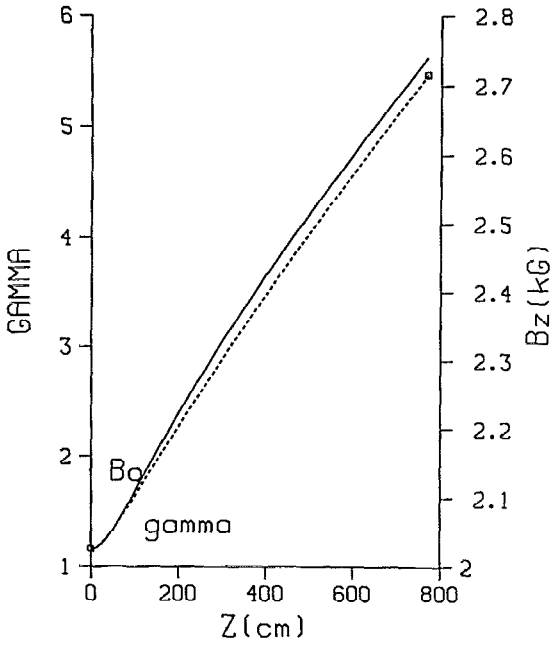

FIG. 2. Results of calculations based on the simplified model of the microwave field. The parameters are: $A=0.01$ cm^{-1} ($E=5.1$ kV/cm), $w=2$ cm^{-1} ($f=9.55$ GHz), Rad $=4$ cm, $v_z/c=0.5$, $\varphi_0=0.8\,\pi$. The energy growth and the magnetic field vs z can also be seen.

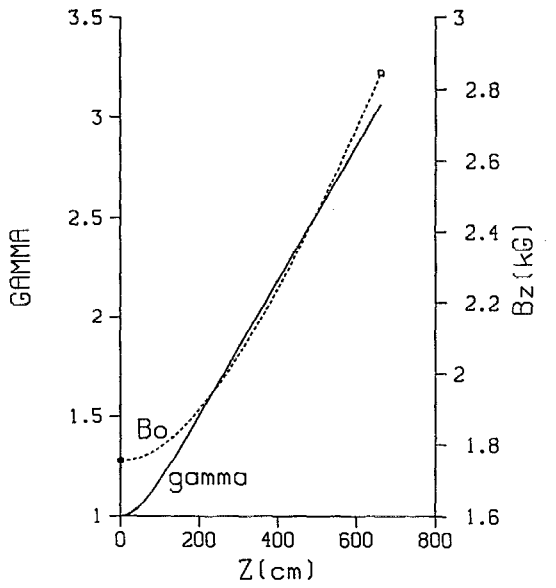

FIG. 3. Calculation results based on the exact waveguide fields. The parameters are the same as in Fig. 2. The energy growth and the magnetic field vs z can also be seen.

As an example, the solution of the complete set of equations in exact fields [see Eq. (1)] for a mildly relativistic beam is shown in Figs. 2 and 3. The parameters used are frequency $=9.55$ GHz, $R=4$ cm, $v_z/c=0.5$, and $A=0.01$ cm^{-1} (about $E=5.1$ kV/cm.) This exact solution is compared to that obtained by solving the simplified set of Eqs. (10)–(14). It is evident that the solutions are right for $\sigma r<1$. This set of numerical solutions is evidence for the validity of the simplified model. Figure 2 is the result of simplified calculations and shows the velocity components, the magnetic field, and the γ factor as functions of z. The corresponding set of the solutions in the exact waveguide fields is given in Fig. 3. It can be seen that for the simplified case, the acceleration is slightly faster. An additional solution for the exact fields is given in Fig. 4 for the case of the electric-field intensity of $E=150$ kV/cm ($A=0.3$ cm^{-1}) and the initial energy of 32 keV. The acceleration takes place in a multimoded waveguide with $R=4$ cm. We see that, if the magnetic field increases to the value of 33 kG, the final energy is about $\gamma=38$ (19 MeV) after about 4 m of acceleration. As also can be seen in the figure, at the advanced acceleration stage, the dependence of the energy on the distance is linear. The main experimental limitation on the final energy value in this case is obviously the magnetic-field magnitude. There seems to be no other limitations as long as the beam current is low enough to ignore space-charge problems and radiation depletion. Figure 5 shows the solution for parameters of the experimental setup: $R=1.92$ cm, $f=8.75$ GHz ($\omega/c=w=1.83$), $A=0.003$ cm^{-1}. After a distance of 1.5 m, the energy anticipated is about $\gamma=1.5$ (250 keV) and the magnetic field increases to a value of 3.3 kG.

III. EXPERIMENTAL SETUP

Figure 6 shows the schematic of the experimental setup. An electron gun, based on a glow argon discharge at 100 mTorr, delivers an electron current of about 1 mA. The electron gun is at a negative potential of 10 kV with respect to the ground circular waveguide. The magnetic field is maintained by discharging a 1500-μF, 4-kV capacitor bank, by means of an ignitron, through the air-cooled solenoids. The pulse length of the magnetic field is about

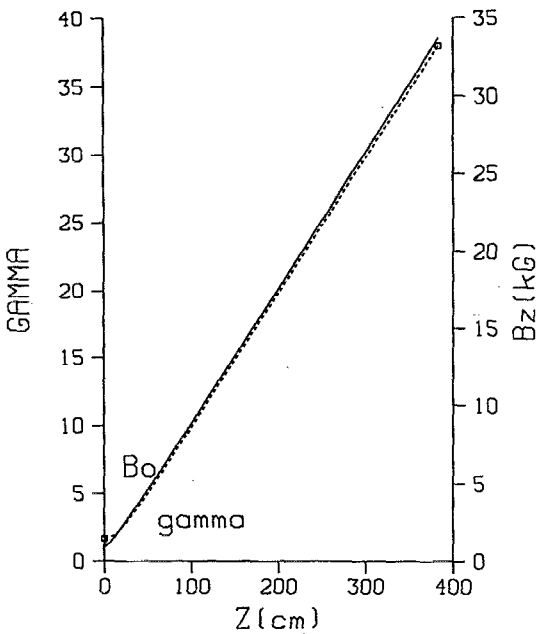

FIG. 4. $A=0.3$ cm^{-1} ($E=150$ kV/cm), $w=2$ cm^{-1}, $R=4$ cm, $v_z/c=0.6$. The energy growth and the magnetic field vs z can also be seen.

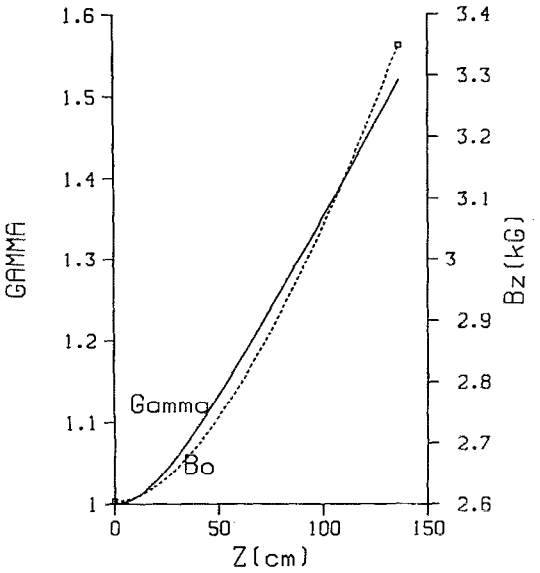

FIG. 5. The e-beam parameters for the experimental setup. $A=0.003$ ($E=1.5$ kV/cm), $w=1.83$ cm^{-1}, $R=1.92$ cm, $v_z/c=0.197$. The energy growth and the magnetic field vs z can also be seen.

20 ms, i.e., quasistatic during the EM radiation pulse. The EM field is produced by a 50-kW peak power, band transmitter. Its pulse width is 2 μs and the pulse repetition frequency (PRF) is 300 Hz. The EM wave frequency was set to 8.755 GHz$\pm$20 MHz. Circular polarization was obtained by means of a turnstile junction.[8] The mismatch of the polarization axis was less than 8%. This method of circular polarization has been chosen because of its tunability, broad bandpass, and low transition losses. It also allows reversal of the polarization rotation direction. X rays are produced by impinging accelerated electrons on a tungsten target and the scattered x rays are sampled through a side window onto a scintillator and a photomultiplier. The angle of the tungsten target is movable and can be set to the most preferable direction. Between the scintillator and the tungsten target absorbing Al or Cu foils of different thickness may be placed.

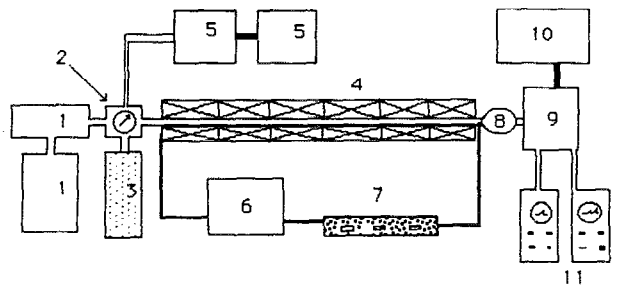

FIG. 6. The schematic of the experimental layout of the autoresonance microwave accelerator. 1: Electron gun system; 2: polarizer; 3: the vacuum system; 4: magnetic coils; 5: the microwave system; 6: capacitor bank; 7: the pulser system; 8: the microwave load; 9: x-ray diagnostics system; 10: MCA; 11: oscilloscopes.

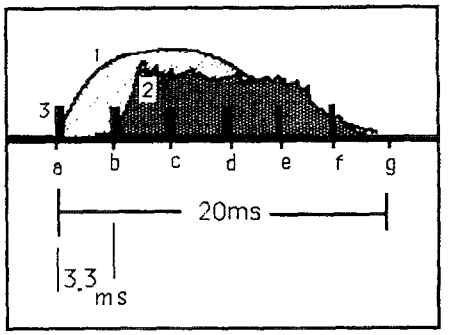

FIG. 7. The relative arrangement of the magnetic-field pulse, the electron beam, and the microwave pulses. 1: the magnetic-field pulse ($\approx$20 ms); 2: the electron-beam current; 3: the microwave pulses (PRF = 300 Hz, PW = 2 μs). It may be seen that the electron beam starts close to the maximum value of the magnetic field and the microwave pulses are 3.3 ms separated apart.

IV. RESULTS AND DISCUSSION

Low beam currents of the order of 300 μA to avoid space-charge effects were used. Theoretical considerations allow continuous acceleration. In the present setup, because of the pulsed nature of the existing magnetic field and the low PRF of the transmitter, only one part in a thousand of the electrons emitted by the gun are accelerated.

One of the most crucial checks of the validity of the acceleration mechanism is obtained by the ability to reverse the direction of the axial magnetic field without changing other parameters. Indeed, when reversing the magnetic-field direction, no x rays have been detected.

The results have been obtained comparing signals of the same x-ray pulse scattered through different absorbers. A typical experimental time dependence of the magnetic field (1), the current (2), and the radiation pulses (3) can be seen in Fig. 7. The repetition rate of the transmitter (300 Hz) allows only three or four radiation pulses to be placed on the magnetic-field pulse. Each microwave radiation pulse interacts with a different level of the magnetic-field intensity.

The EM radiation, the magnetic field, and the beam current are slightly fluctuative and, therefore, statistics of measurements are needed to obtain conclusive results. Only three (the most central) peaks of the transmitted x rays were analyzed. The diagnostic consisted of measuring the half-value levels (HVL) for different pulses (c, d, and e), and finding the average beam energy from Fig. 8 based on Ref. 9.

The results of these measurements are summarized in Fig. 9. It can be seen that the final energies, of channel e, for example, are not at the maximum values, but are much smaller. The reason for this is that each signal is sensing another guide magnetic field and, consequently, is accelerated differently. The maximum energies are detected in

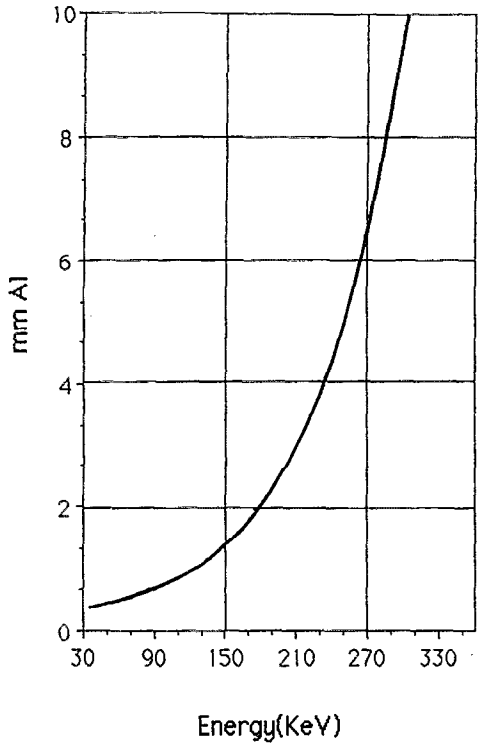

FIG. 8. Graph of the HVL vs the energy of the unfiltered radiation. The beam energy of 100 keV corresponds to HVL of 0.68 mm Al (see Ref. 9).

signals c and d. The signals coming afterwards (b and e) are of energies lower than 100 keV.

The dependence of acceleration on initial energy was also examined. The experiment was designed for accelerating electrons with an initial energy of 10 keV. In Figs.

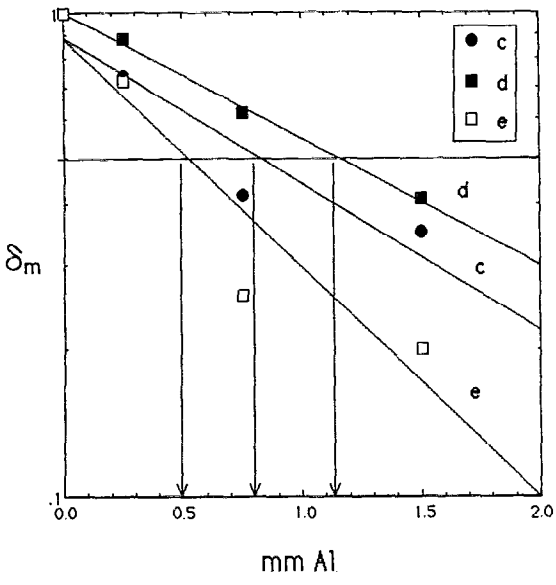

FIG. 9. The half-value level (HVL) as a function of the thickness of the aluminum absorber. At channel d this energy is about 150 keV. On the near channels the achieved energy is a little smaller than on d ($\delta_m = I_m/I_0$).

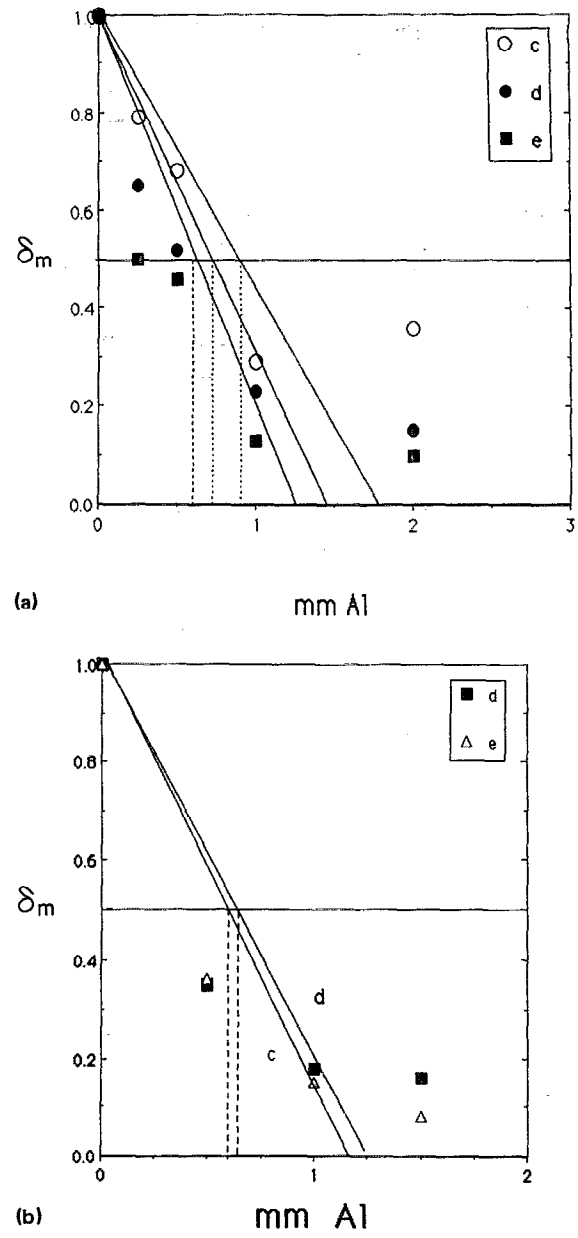

FIG. 10. The half-value level (HVL) functions vs the thickness of the aluminum absorber with inappropriate initial acceleration voltage ($\delta_m = I_m/I_0$). (a) $V_{acc} = 12.5$ kV. The highest achieved energy for channel c is $\approx$110 keV. (b) $V_{acc} = 7.5$ kV. The highest achieved energy is $\approx$70 keV.

10(a) and 10(b) one can see the measured energies for $V_{acc} = 12.5$ kV and $V_{acc} = 7.5$ kV, respectively. In both cases, the highest energy registered was about 0.67 of the maximum values. As has been pointed out earlier, by reversing the direction of the magnetic field, no x rays produced by accelerated electrons were detected.

V. SUMMARY

The autoresonance microwave accelerator (AMA) is capable, in principle, of accelerating electrons to high energies. There may be, however, some obvious limitations such as an impractically high magnetostatic field or EM field intensity. Radiation losses in the proposed scheme are negligible for high energies, because most of the energy is

confined to the axial component of the velocity.[6] Most of the conventional accelerators using microwaves utilize standing EM waves. These schemes require sophisticated focusing devices.[10–12] In our case, focusing is not required, and the electrons move on a stable trajectory in the autoresonance regime.

An additional advantage is due to the fact that we do not need a time-dependent magnetic field (as in the GYRAC concept[13]), and a magnetostatic field is used. Furthermore, the coherent synchrotron radiation properties of the azimuthally bunched beam created in the proposed accelerator could be of considerable interest as a novel coherent radiation source.

ACKNOWLEDGMENTS

The authors would like to thank C. Sharon for his technical assistance, which was crucial for the success of the work.

[1] D. B. McDermott, D. S. Furuno, and N. C. Luhmann, Jr., J. Appl. Phys. **58**, 12 (1985).
[2] K. S. Golovanevsky, IEEE Trans. Plasma Sci. **PS-10**, 120 (1982).
[3] K. S. Golovanevsky, IEEE Trans. Plasma Sci. **PS-11**, 28 (1983).
[4] K. S. Golovanevsky, Sov. J. Plasma Phys. **11**, 174 (1985).
[5] R. Shpitalnik, J. L. Hirshfield, and L. Friedland, Part. Accel. **25**, 1 (1989).
[6] A. Loeb and L. Friedland, Phys. Rev. A **33**, 1828 (1986).
[7] P. Sprangle, L. Vlaos, and C. M. Tang, IEEE Trans. Nucl. Sci. **NS-30**, 3177 (1983).
[8] G. L. Ragan, *Microwave Transmission Circuits* (McGraw-Hill, New York, 1948).
[9] R. Thoraeus, in *A Study of the Ionization Method etc...*, edited by F. Englunds (Boktryckery AB, Stockholm, 1932).
[10] D. L. Judd, Annu. Rev. Nucl. Sci. **8**, 181 (1958).
[11] S. P. Kapitza and V. N. Meleckin, *The Microtron* (Harwood Academic, London, 1978).
[12] L. H. Thomas, Phys. Rev. **54**, 580 (1938).
[13] A. Gal, IEEE Trans. Plasma Sci. **PS-17**, 622 (1989).